

Inclusion of remote sensing information to improve groundwater flow modelling in the Chobe region (Botswana)

**H. J. W. M. HENDRICKS FRANSEN, P. BRUNNER,
L. KGOHLANG & W. KINZELBACH**

*Institute of Hydromechanics and Water Resources Management, ETH-Hönggerberg,
HIL G33.3, CH-8093 Zürich, Switzerland*

hendricks@ihw.baug.ethz.ch

Abstract A groundwater flow model has been built for the Chobe region in Botswana. Due to the scarcity of conventional data, alternative sources of information have been explored. METEOSAT and NOAA-AVHR images have been used to estimate the spatial distribution of the water balance. This spatial distribution has been correlated to local chloride measurements from which the recharge rate could be estimated. A digital elevation model has been used as a constraint for the maximum local piezometric head values. Finally, geomagnetic data were used as an indication for the presence of faults. These data have been used together with a limited number of traditional data (hydraulic head and transmissivity measurements) in an inverse calibration procedure. In the inverse conditioning, equally likely realizations, consistent with all the measurements (transmissivity, hydraulic head, digital elevation model, satellite images, chloride measurements and geomagnetic data) have been generated. The objective function contains an extra constraint on a statistical basis that guarantees that the calibrated recharge rate pattern does not deviate too much from the estimated water balance using the satellite image. The study demonstrates the importance of the digital elevation model and the satellite information in improving the groundwater model of the site.

Keywords conditioning; digital elevation model; geomagnetic data; inverse modelling; remote sensing; spatial patterns

INTRODUCTION

Groundwater flow modelling in semiarid regions in the third world is especially complicated because, as a rule, few data are available and the variability of recharge rates in time and space is very large. In order to build more reliable groundwater flow models for those areas, the value of alternative data sources has to be explored. Satellite images and geophysical images can provide exhaustive information over large areas. They can give imprecise information on geological structures and recharge rate. The information on geological structures can be related to the hydraulic conductivity. The advantage of this kind of information is that it is exhaustive, the disadvantage is that the data are associated with a large measurement error. This poses the question how can these data be used in the calibration of a groundwater model, and whether the data really yield an improvement of the groundwater flow model.

In this paper it is shown that these exhaustive data can be used in the stochastic inverse calibration of a groundwater flow model. Multiple equally-likely realizations

of transmissivity-recharge couples are calculated, which are conditioned to such exhaustive information, namely geomagnetic images, satellite images with water balance information and a digital elevation model. In addition, these realizations are conditioned to transmissivity measurements, hydraulic head data and recharge rate estimates based on the chloride method. This method was applied in the Chobe region in Botswana.

STUDY AREA

The major local geological and topographical features in the study area (the Chobe region in northern Botswana) are the Chobe flood plain, the Chobe forest reserve, the Mababe depression and the Kachikau fault. The Kachikau fault is close to the western and northern boundaries of the study domain. The Chobe flood plain is situated northwest of the fault and the Chobe forest reserve east of it. Both are flat areas. In the extreme southwest of the study region is the Mababe depression. The higher areas (hills) of the region are north of the Mababe depression and in the most eastern part of the study domain.

The following data are available from the area:

- six transmissivity measurements;
- 22 steady-state hydraulic head measurements;
- 16 chloride measurements from which the recharge rate is estimated;
- a digital elevation model;
- METEOSAT images for the period 1995–2000 from which average precipitation (P) is estimated. NOAA-AVHRR images from which average evapotranspiration (ET) is estimated for the period 1990–2000;
- geomagnetic images from which the location of faults is obtained.

APPROACH

The approach used is based on the sequential self-calibrated method. Gómez-Hernández *et al.* (1997) detailed this method for the stochastic inverse modelling of 2-D steady-state groundwater flow. Hendricks Franssen (2001) presented an extension of the methodology for the inverse modelling of 3-D transient groundwater flow (possibly in fractured media) and conservative mass transport. Hendricks Franssen *et al.* (2004) discuss the joint estimation of spatially variable transmissivities and recharge rates. In this study the following procedure has been followed:

- (1) 100 equally likely logtransmissivity (Y) realizations are generated, conditioned to the transmissivity measurements by GCOSIM3D (Gómez-Hernández & Journel, 1993). The mean Y differs slightly between the four different geological zones (including the Kachikau fault). The variogram of Y had to be postulated due to the limited number of measurement data. An exponential model has been taken with an integral scale I_Y equal to 10 km and a sill σ_Y^2 equal to 0.25.
- (2) 100 equally likely recharge rate (R) realizations are generated, on the basis of the chloride measurements and the estimated precipitation minus evapotranspiration

from the METEOSAT and NOAA-AVHR images. The realizations have been generated with the co-located co-simulation algorithm (Almeida & Frykman, 1994). The advantage of this algorithm is that only the linear correlation coefficient between the two variables (the recharge rate estimated from the chloride measurements and $P - ET$ from the satellite images) is needed, and that the algorithm is especially suited for gridded secondary variables. The estimated linear correlation coefficient between the recharge rate estimated by the chloride method and the recharge rate estimated from the satellite images is 0.715 (Brunner *et al.*, 2004). The recharge rate integral scale I_R was estimated from the satellite images ($P - ET$) and found to be 100 km. The nugget and sill of the spherical recharge rate variogram were estimated from the chloride data and set equal to 36 and 394 (mm year^{-1})², respectively.

- (3) The generated Y and R realizations have been used as input to a groundwater flow model. Other input parameters to the groundwater flow model are the external stresses (wells). The boundaries are mostly impervious; at some parts prescribed heads are imposed. The hydraulic head solution is calculated by a finite difference scheme. An objective function is evaluated which contains multiple parts: (a) the sum of squared deviations between measured and simulated heads; (b) the sum of the squared deviations between the simulated piezometric head and the altitude (for all grid cells), in case the piezometric head value is larger than the altitude; and (c) a term that penalizes a too strong deviation of the pattern of the calibrated recharge rates from the $P - ET$ satellite image. In order to formulate statistical bounds on the deviation from the satellite image, 10 000 recharge realizations were generated. 200 control points were randomly located on the simulation domain. A matrix of size 200×200 was built that contains the frequency that the recharge rate at a control point i is larger than the recharge rate at a control point j . The derived frequencies from the 10 000 realizations are therefore estimated probabilities. For each realization the sum of deviations from the mean pattern has been calculated: for instance the probability that the recharge rate at control point 8 is larger than the recharge rate at control point 25 equals 0.7; and the generated recharge rate for a particular realization at control point 8 is larger than the generated recharge rate at control point 25, the contribution to the deviation sum is $(1 - 0.7) = 0.3$. If the generated recharge rate at control point 25 had been larger than the recharge rate at control point 8, this would give a contribution of 0.7. If for all 10 000 realizations the sum of deviations has been calculated, a 95% confidence interval on the sum of deviations can be constructed. The deviation from the pattern is penalized in such a way that calibrated recharge rate patterns that deviate largely from the $P - ET$ image, give an important contribution to the objective function.
- (4) If the calculated objective function value is too large, the spatially variable recharge rate and transmissivity fields are modified. The objective function is minimized with respect to these optimization parameters. The perturbation of the recharge and transmissivity fields is parameterized by selecting a limited number of grid cells (the master blocks) in order to reduce the dimensionality of the optimization problem.
- (5) Step 2 is repeated. The iterative process stops if the objective function value is low enough, or if the maximum number of iterations has been reached.

Steps (1) to (5) are repeated for different scenarios, in order to investigate the impact of the inclusion of different pieces of information. Table 1 summarizes the different scenarios.

For scenarios 1 and 2 the 22 steady-state head data were not used for conditioning. The transmissivity data and information on recharge rate (chloride data and satellite images) were used. The difference between scenarios 1 and 2 is that in scenario 2 the digital elevation model has been used as conditioning information (giving a constraint on the maximum piezometric head value). In scenarios 3 to 10, hydraulic head data are used for inverse conditioning. For scenarios 5 to 10 an additional constraint is included regarding the pattern of calibrated recharge rates.

Table 1 The different scenario studied.

Scenario	Head data?	DEM?	Patterns?	Faults?	Many faults?
1	No	No	No	No	No
2	No	Yes	No	No	No
3	Yes	No	No	No	No
4	Yes	Yes	No	No	No
5	Yes	No	Yes	No	No
6	Yes	Yes	Yes	No	No
7	Yes	No	Yes	Yes	No
8	Yes	Yes	Yes	Yes	No
9	Yes	No	Yes	No	Yes
10	Yes	Yes	Yes	No	Yes

For scenarios 7 and 8 geomagnetic information is used to determine the position of faults. These faults are treated as one additional geological zone. An alternative approach is to treat each fault as a separate geological zone. This is done in scenarios 9 and 10 and gives rise to 19 additional zones (23 zones in total).

For each scenario, ensemble statistics are calculated over the 100 conditioned realizations. The ensemble average transmissivity and recharge rate are calculated for each active grid cell, and also over all active grid cells. The ensemble standard deviation is evaluated by:

$$AESD(X) = \frac{1}{N} \sum_{i=1}^N \sigma_{X_i}$$

where $AESD$ is the average ensemble standard deviation, X is recharge rate, transmissivity or hydraulic head, N is the number of active grid cells and σ_{X_i} the standard deviation for recharge rate, logtransmissivity or hydraulic head for an active grid cell i .

RESULTS

Table 2 gives the ensemble statistics for the different scenarios. Given are the ensemble average log-transmissivity, the ensemble standard deviation of log-transmissivity, the

ensemble average recharge rate, the ensemble recharge rate standard deviation and the ensemble standard deviation of hydraulic head.

Table 2 The calculated ensemble statistics for the different scenarios, given in Table 1.

Scenario	Average Y $\log(\text{m}^2 \text{s}^{-1})$	$AESD(Y)$ $\log(\text{m}^2 \text{s}^{-1})$	Average R (mm year ⁻¹)	$AESD(R)$ (mm year ⁻¹)	$AESD(h)$ (m)
1	-3.53	0.45	13.8	9.0	3083.6
2	-1.71	0.68	6.0	4.0	6.4
3	-2.31	0.74	9.0	5.4	454.3
4	-2.38	0.61	6.4	3.3	10.3
5	-2.29	0.72	8.5	5.2	244.3
6	-2.25	0.67	6.9	4.3	11.2
7	-2.24	0.73	8.1	5.6	218.1
8	-2.17	0.68	6.8	4.7	14.4
9	-2.51	0.63	7.2	6.6	198.6
10	-2.36	0.59	6.4	4.7	14.4

The following can be learned from the results. For scenario 1, where we use only transmissivity and recharge rate data, the hydraulic head values are too large; the hydraulic head is far above the terrain on many locations in many realizations. As a consequence, conditioning to the digital elevation model results in a strong increase of the transmissivity, and a decrease of the average recharge rate. The recharge rate decreases by about 60% (a factor of 2.5) whereas the transmissivity increases by a factor of 60. The recharge rate is modified less as it is more constrained by the available information. The conditioning results in an increased spatial variability of transmissivity, and a decreased spatial variability of recharge rate. The uncertainty in the estimated hydraulic heads decreases strongly, as could be expected.

The simulations also show that conditioning to hydraulic heads only, and not to the digital elevation model, can not avoid large areas where the piezometric head is above the terrain. If both the piezometric head data and the digital elevation model are used as conditioning information, the uncertainty of transmissivity and recharge rate are smaller than in the case that only the digital elevation model was used. The increase of transmissivity is reduced when hydraulic head data are used for conditioning. It is likely that conditioning to the digital elevation model resulted in a modification so that in the first iteration the piezometric head is everywhere below the terrain. However, at many locations the piezometric head may have been lowered excessively. The piezometric head measurements allow correction of this, resulting in a reduced transmissivity increase (about a factor of 15).

For all the other scenarios we see that a digital elevation model always reduces the ensemble variance (compare the $AESD(X)$ for scenario 6 with those for scenario 5, and similarly those for scenario 8 with scenario 7, and those for scenario 10 with those for scenario 9).

The inclusion of an additional part to the objective function, that monitors the modification of the recharge rate pattern and penalizes too large deviations from it, has no significant impact on the calculated ensemble statistics. However, something interesting can be noticed here that proves the value of the satellite images: for 99 out

of 100 realizations (data not presented) the recharge rate pattern after conditioning to hydraulic heads (scenario 5) was closer to the $P - ET$ image from the satellite than before inverse conditioning (scenario 1). The additional part in the objective function was never “activated”, and so it is concluded that only the piezometric head data directed the solution that resembles the satellite image more closely. The additional constraining of the inverse solution of the groundwater flow equation by means of the digital elevation model (scenario 6) yielded, for 88 out of 100 realizations, a calibrated recharge rate pattern that was even closer to the pattern of the $P - ET$ image. These results indicate that we were too pessimistic about the quality of the $P - ET$ image in the stochastic generation of the recharge rate fields. The 100 recharge rate fields, generated by the co-located co-simulation algorithm, deviated too much from the original image, based on a too pessimistic perception of the image quality.

Finally, the inclusion of geomagnetic information has been investigated. No important tendencies can be detected in the ensemble statistics. However, for scenarios 9 and 10 (many faults that are treated as separate geological zones) the average log-transmissivity increases less than compared to scenario 1 (for scenario 9 only by a factor of 10). However, it cannot be proven that this is realistic. Actually, we do not have enough information to pose realistic constraints on maximum and minimum possible transmissivities in the faults. It is interesting to see that after the inverse calibration some faults have a clearly larger transmissivity, while for most of the faults the transmissivity after calibration is close to the prior transmissivity.

Figure 1 gives some figures for one of the scenarios studied, scenario 6.

CONCLUSIONS AND DISCUSSION

A methodology has been presented that is able to incorporate exhaustive information from images (satellite images, geophysical survey) as conditioning information in stochastic inverse models. The stochastic inverse modelling produces multiple equally likely realizations that are conditional to this information, besides being conditional to traditional information such as transmissivity measurements, hydraulic head measurements and recharge rate estimations by the chloride method. The method has been applied in the Chobe region and the worth of a digital elevation model as conditioning information was evident. It was also demonstrated that METEOSAT and NOAA-AVHR images contained relevant information for improving the characterization of the spatially variable recharge rate. Also, geomagnetic information was used to identify geological structures. It could not be clarified whether the use of this information in inverse models improved the characterization of groundwater flow.

The value of geomagnetic information will be subject to future research. Also, scenarios with a cross-correlation between transmissivity and recharge rate will receive attention, as it is likely that there is some degree of correlation. The possibility that there are areas with a negative recharge rate, due to transpiration from trees, will be a third subject for future research. Additional satellite information will be studied and possibly included in the conditioning process in order to identify such areas.

The conditioning to pattern information is a topic of continuing research.

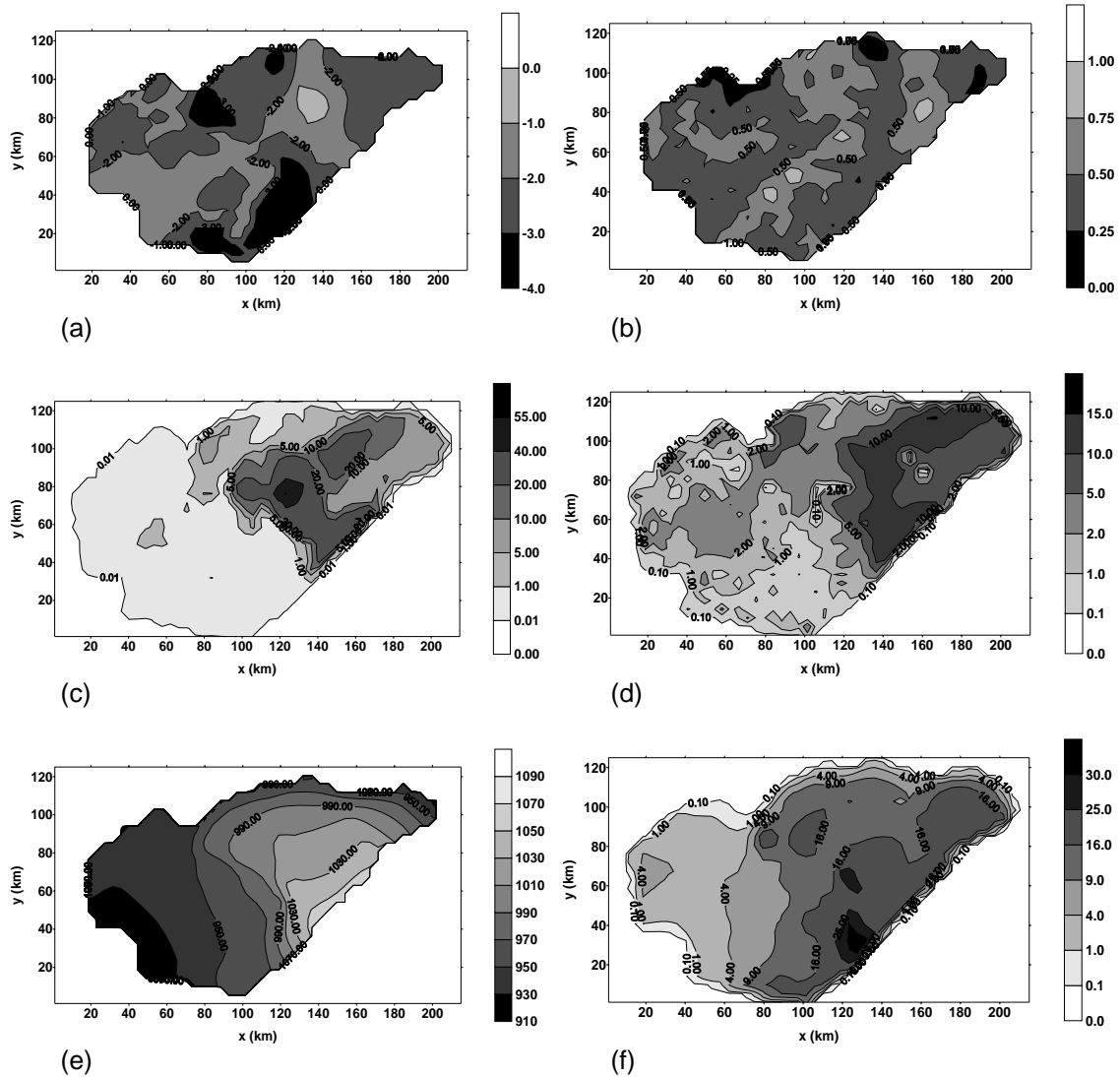


Fig. 1 For scenario 6: (a) average log-transmissivity Y ; (b) standard deviation of Y ; (c) average recharge rate R ; (d) standard deviation of R ; (e) average head; and (f) standard deviation of head.

REFERENCES

- Almeida, A. S. & Frykman, P. (1994) Geostatistical modeling of Chalk properties in the Dan Field, Danish North Sea. In: *Stochastic Modeling and Geostatistics* (ed. by J. M. Yarus & R. L. Chambers). AAPG Computer Applications in Geology, no. 3. AAPG, Tulsa, Oklahoma, USA.
- Brunner, P., Bauer, P., Eugster, M. & Kinzelbach, W. (2004) Using remote sensing to regionalize local precipitation recharge rates obtained from the Chloride Method. *J. Hydrol.* **294**, 241–250.
- Gómez-Hernández, J. J. & Journel, A. G. (1993) Joint sequential simulation of multi-Gaussian fields. In: *Geostatistics Troia'92*, vol. 1 (ed. by A. Soares), 85–94. Kluwer Academic Publishers, Dordrecht, The Netherlands.
- Gómez-Hernández, J. J., Sahuquillo, A. & Capilla, J. E. (1997) Stochastic simulation of transmissivity fields conditional to both transmissivity and piezometric data. 1. Theory. *J. Hydrol.* **203**(1–4), 162–174.
- Hendricks Franssen, H. J. W. M. (2001) Inverse stochastic modelling of groundwater flow and mass transport. PhD Thesis. Technical University of Valencia, Spain.
- Hendricks Franssen, H. J., Stauffer, F. & Kinzelbach, W. (2004) Joint estimation of transmissivities and recharges-application: stochastic characterization of well capture zones. *J. Hydrol.* **294**, 87–102.